Kinetics and Mechanism of Water Substitution at Half-Sandwich Iridium(III) Aqua Cations $Cp^*Ir(A-B)(H_2O)^{2+/+}$ in Aqueous Solution ($Cp^* = \eta^5$-Pentamethylcyclopentadienyl Anion; $A-B$ = Bidentate N,N or N,O Ligand)

Tilo Poth,[a] Helmut Paulus,[c] Horst Elias,*[a] Carlos Dücker-Benfer,[b] and Rudi van Eldik[b]

Keywords: Iridium / Sandwich complexes / Kinetics / N ligands / Reaction mechanisms

The perchlorate complexes of a series of half-sandwich monoaqua cations $Cp^*Ir(A–B)(H_2O)^{2+/+}$ with A–B = prol (D/L-proline anion), picac (picolinic acid anion), *R,R*-dach [(–)-(1*R*,2*R*)-1,2-diaminocyclohexane], *R,R*-dpen [(+)-(1*R*,2*R*)-1,2-diphenylethylenediamine], phen (*o*-phenanthroline), and bpy (2,2′-bipyridine) ($Cp^* = \eta^5$-pentamethylcyclopentadienyl anion) have been prepared and characterized. An X-ray structure analysis of $Cp^*Ir(R,R\text{-dach})(H_2O)(ClO_4)_2\cdot H_2O$ has revealed that the cation $Cp^*Ir(R,R\text{-dach})(H_2O)^{2+}$ has a distorted pseudo-octahedral coordination geometry. In the case of A–B = prol, crystallization from water led to the trinuclear complex $[Cp^*Ir(\text{D-prol})]_3(ClO_4)_3$, which has also been characterized by X-ray structure analysis. The experimental data suggest that in aqueous solution the trinuclear proline complex dissociates to form the cation $Cp^*Ir(\text{D-prol})(H_2O)^+$. The proton dissociation constants of the coordinated water in $Cp^*Ir(A–B)(H_2O)^{2+/+}$ have been determined as $pK_a = 7.5$ (A–B = bpy) and $pK_a = 7.1$ (A–B = *R,R*-dach and picac). Substitution of the water in $Cp^*Ir(A–B)(H_2O)^{2+/+}$ by the monodentate ligands L = py (pyridine), DMS (dimethyl sulfide), TU (thiourea), and monodentate anions according to the Equation $Cp^*Ir(A–B)(H_2O)^{2+/+} + L \rightarrow Cp^*Ir(A–B)L^{2+/+} + H_2O$ has been studied by multi-wavelength stopped-flow spectrophotometry in aqueous solution at $I = 0.2$ M. This kinetic investigation, carried out at different concentrations, temperatures, and pressures, showed that the process obeys second-order kinetics, where rate = $k_L[Cp^*Ir(A–B)H_2O^{2+/+}][L]$. The magnitude of the second-order rate constant k_L depends on the nature of both A–B and L. The data for k_L have been found to range from 6.4×10^4 $M^{-1}s^{-1}$ (A–B = D-prol; L = TU) to 10.5 $M^{-1}s^{-1}$ (A–B = bpy; L = py) at 298 K. The activation parameters for water substitution at $Cp^*Ir(A–B)(H_2O)^{2+/+}$ (A–B = bpy, *R,R*-dach, and picac) by L = TU have been evaluated. The activation volumes of $\Delta V^{\neq}$ = +2.3, +7.4, and +7.3 cm^3 mol^{-1}, respectively, are supportive of an I_d mechanism. The results regarding the kinetic lability of the coordinated water in the monoaqua cations $Cp^*Ir(A–B)(H_2O)^{2+/+}$ are compared to those obtained for the triaqua cation $Cp^*Ir(H_2O)_3^{2+}$.

Introduction

The aqua cations $Cp^*Rh(H_2O)_3^{2+}$ and $Cp^*Ir(H_2O)_3^{2+}$ (**1**) belong to the small group of water-stable organometallic species in which water molecules and carbocyclic ligands, such as π-Cp* (= η^5-pentamethylcyclopentadienyl anion), are bound to the same metal centre.[1] There has been a wide spectrum of studies on the chemistry of these aqua cations, providing insight into the relatively new field of aqueous organometallic chemistry.[2−6]

Our interest in half-sandwich aqua cations lies mainly in their intriguing kinetic properties. The introduction of the Cp* group into the cation $Ir(H_2O)_6^{3+}$ leads to a dramatic increase of 14 orders of magnitude in the rate of water exchange, as described by rate constant k_{ex} in Equation (1), and in the rate of water substitution, as described by rate constant k_f in Equation (2) (L = monodentate ligand).[7−12]

$$Cp^*Ir(H_2O)_3^{2+} + H_2O^* \overset{k_{ex}}{\rightleftharpoons} Cp^*Ir(H_2O)^*(H_2O)_2^{2+} + H_2O \qquad (1)$$

$$Cp^*Ir(H_2O)_3^{2+} + L \underset{k_r}{\overset{k_f}{\rightleftharpoons}} Cp^*Ir(H_2O)_2L^{2+} + H_2O \qquad (2)$$

Replacement of two of the coordinated water molecules in the cation **1** by bidentate ligands A−B generates the monoaqua species $Cp^*Ir(A-B)(H_2O)^{2+/+}$. The literature on such iridium compounds is still very limited,[13] but numerous examples of the monochloro analogues $Cp^*Ir(A-B)Cl^{+/0}$ have been described. These species have been found to be particularly effective as catalysts[14−19] and in the coordination of biologically important molecules.[20]

As an extension of our earlier work on the kinetics of Equations (1) and (2),[7,8] we now compare the labilizing effect of the Cp* group, as documented by the rate data available for Equations (1) and (2), with that of bidentate ligands A−B in the monoaqua species $Cp^*Ir(A-B)(H_2O)^{2+/+}$. The kinetics of water substitution according to Equation (3) have been studied in aqueous solution using a series of complexes $Cp^*Ir(A-B)(H_2O)^{2+/+}$

---

[a] Institut für Anorganische Chemie, Technische Universität Darmstadt,
Petersenstraße 18, 64287 Darmstadt, Germany
E-mail: elias@tu-darmstadt.de
[b] Institut für Anorganische Chemie, Universität Erlangen-Nürnberg,
Egerlandstraße 1, 91058 Erlangen, Germany
[c] Technische Universität Darmstadt, Fachbereich Materialwissenschaft
64287 Darmstadt, Germany

Supporting information for this article is available on the WWW under http://www.wiley-vch.de/home/eurjic or from the author.

1434−1948/01/0505−1361 $ 17.50+.50/0

Table 1. Abbreviations used for the aqua complexes

$Cp^*Ir(H_2O)_3{}^{2+}$	**1**	$[Cp^*Ir(bpy)(H_2O)](ClO_4)_2$	**5b**
$Cp^*Ir(R,R\text{-dach})(H_2O)^{2+}$	**2**	$Cp^*Ir(picac)(H_2O)^+$	**6**
$[Cp^*Ir(R,R\text{-dach})(H_2O)](ClO_4)_2\cdot H_2O$	**2b**	$[Cp^*Ir(piac)]_3(ClO_4)_3$	**6b**
$[Cp^*Ir(\text{D-prol})]_3{}^{3+}$	**3**	$Cp^*Ir(R,R\text{-dpen})(H_2O)^{2+}$	**7**
$[Cp^*Ir(\text{D-prol})]_3(ClO_4)_3$	**3b**	$[Cp^*Ir(R,R\text{-dpen})(H_2O)](ClO_4)_2$	**7b**
$Cp^*Ir(\text{D-prol})(H_2O)^+$	**4**	$Cp^*Ir(phen)(H_2O)^{2+}$	**8**
$Cp^*Ir(bpy)(H_2O)^{2+}$	**5**	$[Cp^*Ir(phen)(H_2O)](ClO_4)_2$	**8b**

(**2**, **4−8**) containing neutral or anionic N,N and N,O ligands A−B (see Scheme 1). The incoming ligands L used in the study of the reaction according to Equation (3) have been either neutral species (py, py-nia, DMS, TU)[21] or anions (Br^-, I^-, SCN^-, $N_3{}^-$, $NO_2{}^-$).

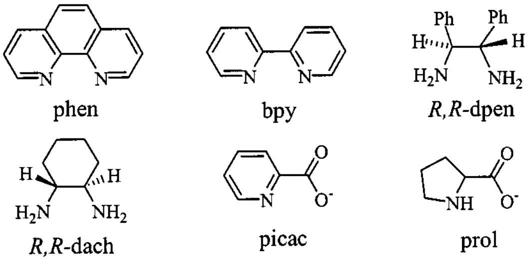

Scheme 1. Bidentate ligands A−B coordinated in monoaqua complexes $Cp^*Ir(A{-}B)(H_2O)^{2+/+}$ and abbreviations[21]

$$Cp^*Ir(A\text{-}B)(H_2O)^{2+/+}\ L \underset{k_{-L}}{\overset{k_L}{\rightleftharpoons}} Cp^*Ir(A\text{-}B)L^{2+/+} + H_2O \tag{3}$$

The present contribution summarizes the kinetic results obtained at various temperatures and pressures. We also present crystallographic data for the perchlorates of the cations $Cp^*Ir(R,R\text{-dach})(H_2O)^{2+}$ (**2**) and $[Cp^*Ir(prol)]_3{}^{3+}$ (**3**) (*R*,*R*-dach = 1,2-diaminocyclohexane; prol = anion of proline)[21] as well as acidity constants (pK_a) for the coordinated water in some of the mono aqua cations $Cp^*Ir(A{-}B)(H_2O)^{2+/+}$.

Results and Discussion

Properties of the Monoaqua Species $Cp^*Ir(A{-}B)(H_2O)^{2+/+}$

The UV spectra of aqueous solutions of the perchlorates of the cations $Cp^*Ir(A{-}B)(H_2O)^{2+/+}$ led to the absorption data listed in Table 2. The various cations absorb in the range 260−320 nm with absorptivities ε_{max} of the order of 10^3 $M^{-1}cm^{-1}$ in the case of aliphatic ligands A−B (dach, dpen, prol)[21] and 10^4 $M^{-1}cm^{-1}$ in the case of aromatic ligand systems (bpy, phen, picac).[21] In the case of the proline complex, the spectra were recorded using solutions of the trinuclear complex **3b**. However, the spectral data strongly suggest that the trinuclear complex dissociates to form the monoaqua cation $Cp^*Ir(\text{D-prol})(H_2O)^+$ (**4**). This follows from the fact that (i) the data for ε_{max}, when referenced to **4** instead of **3**, are close to those obtained for the other mono aqua species, and (ii) the data obtained for ε_{max} at pH = 2.0, 4.8, and 6.0 are identical.

Table 2. UV absorption $\{\lambda_{max}$ [nm] (ε_{max} [$M^{-1}cm^{-1}$])$\}$ of the cations $Cp^*Ir(A{-}B)(H_2O)^{2+/+}$ in aqueous solution at pH = 2.0 and 293 K

5 (A−B = bpy)	243 (15500), 308 (13500), 317 (13400)
8 (A−B = phen)	298 (4990), 276 (16100), 218 (13200), 201 (16500)
2 (A−B = *R*,*R*-dach)	269 (2070), 302 (1660)
7 (A−B = *R*,*R*-dpen)	265 (1690), 298 (1080)
4 (A−B = D-prol)	282 (1160), 300 (1150)[a][b]
6 (A−B = picac)	311 (4740), 260 (10600)

[a] The data obtained at pH = 6 are identical to those obtained at pH = 2.0. − [b] The values of λ_{max} and ε_{max} refer to 1 mol of **4**, not to 1 mol of **3**.

The spectral changes associated with substitution reaction according to Equation (3) are sufficient to allow reliable spectrophotometric monitoring. As an example, Figure 1 shows a series of spectra describing the reaction of **2** with bromide ions according to Equation (3). The existence of two sharp isosbestic points (at 257 nm and 267 nm) indicates that the reaction does not involve substantial concentrations of intermediates.

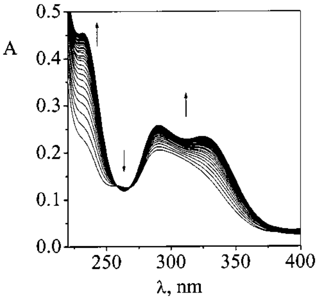

Figure 1. Spectral changes recorded for the reaction of **2** with bromide ions according to Equation (3) within 1.2 s $\{[\text{complex}]_o = 1.0 \times 10^{-4}$ M, $[Br^-]_o = 1.0 \times 10^{-3}$ M; pH = 2.0 ($HClO_4$), $I = 0.2$ M ($NaClO_4$), 298 K$\}$

It is well documented that, due to proton dissociation from coordinated water, aqueous solutions of the triaqua iridium species **1** are acidic.[9] For comparison purposes, the acid dissociation of some of the monoaqua species $Cp^*Ir(A{-}B)(H_2O)^{2+/+}$ according to Equation (4) was therefore investigated by means of spectrophotometric titrations. The pK_a values presented in Table 3 show that (i) the effect of the nature of the bidentate ligand A−B and of the overall charge of the cation on the pK_a is very minor, and (ii) the dissociation constant K_a of the monoaqua species is more than three orders of magnitude smaller than that of the triaqua species **1**. The chelate ligands A−B presumably reduce the electrophilicity of the Ir^{III} centre, such that less electron density is donated by the water oxygen atom. The coordinated water molecule thus becomes a weaker acid.

Table 3. Acidity constants pK_a of the monoaqua species $Cp^*Ir(A-B)(H_2O)^{2+/+}$ at 298 K (I = 0.2 M)

Complex	pK_a
5	7.5 ± 0.2[a]
2	7.1 ± 0.5
6	7.1 ± 0.5
1 [= $Cp^*Ir(H_2O)_3^{2+}$]	3.86 ± 0.03[b]

[a] Taken from ref.[7] – [b] Taken from ref.[9]

At pH ≤ 5, the formation of monohydroxo species $Cp^*Ir(A-B)(OH)^{+/0}$ can be neglected.

$$Cp^*Ir(A\text{-}B)(H_2O)^{2+/+} \overset{K_a}{\rightleftharpoons} Cp^*Ir(A\text{-}B)(HO)^{+/0} + H^+ \tag{4}$$

Structures of the Complexes 2b and 3b

To the best of our knowledge, **2b** represents the first structurally characterized monoaqua half-sandwich iridium Cp* complex of the type $Cp^*Ir(A-B)(H_2O)^{2+}$. As shown in Figure 2, the coordination geometry of the cation **2** is of the "three-legged piano stool" type[22] and can be classified as pseudo-octahedral. The perchlorate ions are disordered and the single water molecule of crystallization is far away from the coordination sphere of the iridium centre.

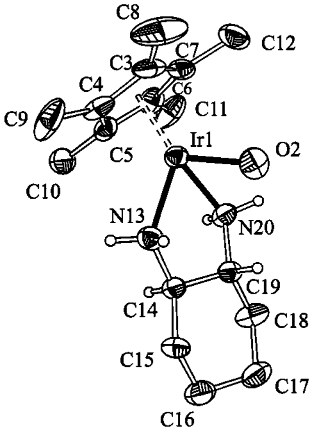

Figure 2. Molecular structure of the cation **2** with thermal ellipsoids drawn at a 30% probability level; most of the hydrogen atoms have been omitted for the sake of clarity

The crystal contains two crystallographically distinct units of **2**. The difference is small and is manifested, for example, in the relative positions of the Cp* and cyclohexane rings. In unit I, the angle between the plane of the Cp* ring and the plane formed by the donor atoms N13, N20, and O2 amounts to 2.7°. In unit II, this angle is found to be just 1.0°.

The bond lengths N13–Ir1 (2.127 Å) and N20–Ir1 (2.130 Å) are very similar (see Table 4), while the bond length O2–Ir1 is slightly longer (2.18 Å). The $Ir-OH_2$ bond length of 2.18 Å is significantly longer than those reported for other Ir^{III} aqua complexes, which range from 2.057 Å for oxo-bridged trinuclear iridium hexacarboxylate complexes to 2.074 Å for hydroxo-bridged bis(ethylenediamine)iridium complexes.[23,24] This ground-state bond lengthening must be due to the *trans* influence of the Cp* ligand and may account for the high lability of the coordinated water molecule. Ir–O distances in the even more labile cation **1** (longest distance 2.27 Å[6]) are in line with this conclusion. By comparison, the water exchange at $Ir(H_2O)_6^{3+}$ is 10^{14} times slower than that at **1**.[7,10] The bond angles N20–Ir1–N13, N20–Ir1–O2, and N13–Ir1–O2 in **2** are close to 80°, which indicates the deviation from ideal octahedral geometry of 90°. The iridium atom is a centre of asymmetry, but the C_2 symmetry of the ligand *R*,*R*-dach brings about a definite, nonracemic configuration.

Table 4. Selected bond lengths and angles in unit I of the complex **2b**

Atoms	Distance [Å]	Atoms	Angle [°]
Ir(1)–N(20)	2.127(8)	N(20)–Ir(1)–N(13)	79.0(3)
Ir(1)–N(13)	2.130(8)	N(20)–Ir(1)–O(2)	80.9(3)
Ir(1)–O(2)	2.180(7)	N(13)–Ir(1)–O(2)	83.6(3)
Ir(1)–C(3)	2.180(9)	X1a–Ir(1)–O(2)[a]	128.7(3)
Ir(1)–C(4)	2.143(12)	X1a–Ir(1)–N(13)[a]	132.0(4)
Ir(1)–C(5)	2.113(9)	X1a–Ir(1)–N(20)[a]	133.0(4)
Ir(1)–C(6)	2.178(9)	C(19)–N(20)–Ir(1)	110.2(5)
Ir(1)–C(7)	2.170(9)	C(19)–C(14)–N(13)	108.9(6)
Ir(1)–X1a[a]	1.777(2)	C(14)–N(13)–Ir(1)	111.9(5)
N(13)–C(14)	1.502(9)	C(14)–C(19)–N(20)	108.1(6)
C(19)–N(20)	1.510(9)	C(4)–Ir(1)–C(3)	39.6(6)
C(14)–C(19)	1.457(10)	C(5)–Ir(1)–C(4)	41.1(4)
C(3)–C(7)	1.45(2)	C(5)–Ir(1)–C(6)	38.3(4)
		C(7)–Ir(1)–C(6)	36.5(4)
		C(7)–Ir(1)–C(3)	38.9(5)

[a] The position X1a corresponds to the center of the Cp* ring.

While this work was being carried out, a series of complexes containing trinuclear units $[Cp^*M(aa)]_3^{3+}$ (M = Rh, Ir; aa = amino acid anion) was reported.[3,15,25] All of these complexes were obtained by crystallization from methanol. With regard to aqueous solutions, the possibility of trimer dissociation and the formation of mononuclear $Cp^*M(aa)(H_2O)^+$ units has yet to be fully explored.

In the presence of perchlorate ions, crystallization from an acidic aqueous solution of the cation **4** leads to yellow prisms, which are structurally composed of trinuclear units **3** with C_3 symmetry (see Figure 3). The structural backbone of these units is a 12-membered metallacycle, consisting of three iridium atoms and three doubly *O*-bonded carboxylate groups. The pseudo-octahedral coordination sphere about each iridium atom is made up by the η^5-bound Cp* ring, one *N*,*O*-bound proline, and another *O*-bound proline. As shown in Table 5, the Ir1–O18 bond to the *N*,*O*-bound proline (2.138 Å) is slightly longer than the Ir1–O19A bond to the singly coordinated neighbouring proline (2.108 Å).

The trinuclear unit 3 possesses 3 × 3 chiral centres (Ir, N, α-C) and the diastereomer within the crystal has to be described as ($R_CR_CR_C$,$R_NR_NR_N$,$R_{Ir}R_{Ir}R_{Ir}$)-**3b**. The unit is the mirror image of the (all-*S*)-configured analogue reported by Beck and co-workers.[26] The chirality at the metal centre is determined by the configuration of the

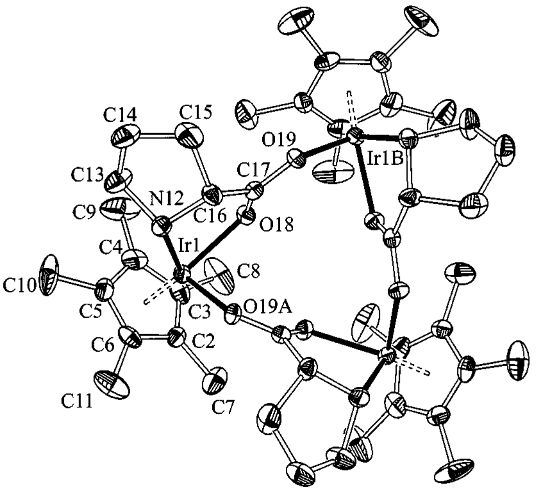

Figure 3. Molecular structure of the trinuclear cation **3** with thermal ellipsoids drawn at a 30% probability level; hydrogen atoms have been omitted for the sake of clarity

Table 5. Selected bond lengths and angles in the complex **3b**

Atoms	Distance [Å]	Atoms	Angle [°]
Ir(1)−O(19A)[a]	2.108(6)	O(19)−Ir(1)−O(18)	81.5(3)
Ir(1)−N(12)	2.136(8)	N(12)−Ir(1)−O(18)	76.8(4)
Ir(1)−O(18)	2.138(5)	O(19)−Ir(1)−N(12)	78.7(3)
Ir(1)−C(6)	2.099(10)	X1a−Ir(1)−N(12)[b]	134.5(5)
Ir(1)−C (4)	2.100(11)	X1a−Ir(1)−O(18)[b]	134.9(5)
Ir(1)−C(5)	2.133(12)	X1a−Ir(1)−O(19)[b]	128.7(5)
Ir(1)−C(2)	2.133(10)	Ir(1)−N(12)−C(16)	112.2(6)
Ir(1)−C(3)	2.140(12)	Ir(1)−O(18)−C(17)	115.0(7)
Ir(1)−X1a[b]	1.754(10)	Ir(1B)−O(19)−C(17)[c]	127.6(5)
N(12)−C(16)	1.484(12)	N(12)−C(16)−C(17)	108.7(8)
C(16)−C(17)	1.503(13)	C(16)−C(17)−O(18)	121.4(8)
C(17)−O(18)	1.249(13)	C(16)−C(17)−O(19)	114.6(7)
C(17)−O(19)	1.284(11)	Ir(1)−N(12)−C(13)	117.1(7)

[a] O(19A): O(19) transformed to $1 - x + y$, $1 - x$, z. − [b] The position X1a corresponds to the center of the Cp* ring. − [c] Ir(1B): Ir(1) transformed to $1 - y$, $x - y$, z.

asymmetric carbon atom, making the complex an example of chiral self-recognition.

Kinetics of Water Substitution

A kinetic investigation of water substitution according to Equation (3) was undertaken to study the reactivity and mechanistic behaviour of the coordinated water in the monoaqua species $Cp^*Ir(A-B)(H_2O)^{2+/+}$ and to compare it with that in the triaqua species **1**. We recently reported that water substitution at the triaqua species follows an I_d mechanism[21] with the rate of substitution being close to the rate of water exchange.[9] For a variety of $Cp^*Ir(A-B)(H_2O)^{2+/+}/L$ systems, systematic variation of A−B (with L = constant) and of L (with A−B = constant) was carried out to obtain detailed information on the effect of the bidentate ligands A−B on the kinetics and mechanism of the reaction according to Equation (3).

Water Substitution in Complexes $Cp^*Ir(A-B)(H_2O)^{2+/+}$ by Pyridine

In a series of experiments, water substitution in six monoaqua $Cp^*Ir(A-B)(H_2O)^{2+/+}$ complexes by pyridine was investigated at pH = 2.0 and 4.8. These substitution reactions were expected to be second-order processes. Accordingly, under pseudo-first-order conditions the change of absorbance with time was found to be monophasic and exponential. Fitting of Equation (5) to the (A,t) data led to the observed rate constant k_{obsd} (ΔA = amplitude). As an example, Figure 4a shows the dependence of k_{obsd} on $[py]_{tot}$ for the system **4**/py.

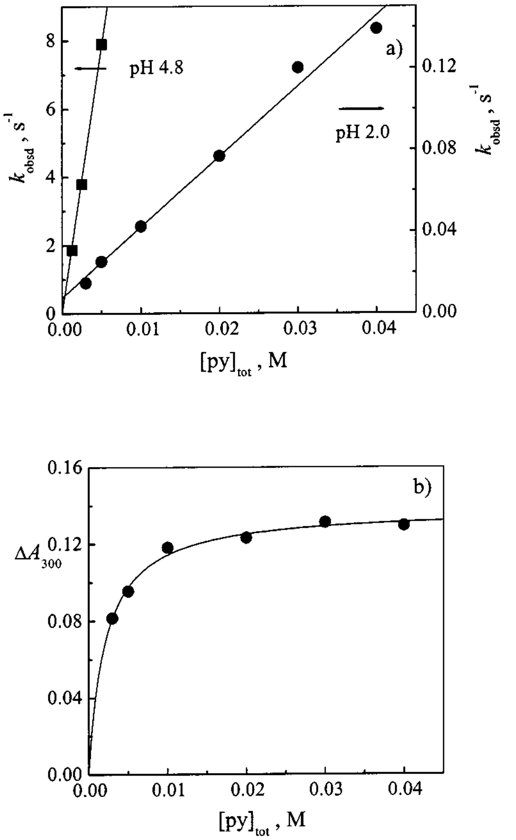

Figure 4. Dependence of the kinetic parameters k_{obsd} (a) and ΔA_{300} (b) on $[py]_{tot}$ for the reaction of the cation **4** with pyridine at pH = 2.0 and 4.8

$$A = \Delta A \exp(-k_{obsd}t) + A_{\infty} \quad (5)$$

$$k_{obsd} = k_L[py] = m[py]_{tot} \quad (6)$$

$$k_{obsd} = k_L[py] + k_{-L} = m[py]_{tot} + k_{-L} \quad (7)$$

At pH = 4.8, the dependence is linear and conforms to Equation (6) (irreversible pseudo-first-order reaction), whereas at pH = 2.0 the linear dependence has an intercept and conforms to Equation (7) (reversible pseudo-first-order reaction).[27] The slope m of the linear dependencies shown in Figure 4a leads to rate constant k_L and the intercept corresponds to k_{-L}.[28] At pH = 2.0, where most of the pyridine is protonated ($pK_a = 5.26$[29]), the reverse reaction (rate constant k_{-L}) is observed and the equilibrium constant K is obtained from the ratio k_L/k_{-L}. Independently and additionally, K can be derived from the concentration dependence of the amplitude ΔA, as described by Equation (8) and shown in Figure 4b.

Table 6. Rate constants k_L and k_{-L} and equilibrium constants K for water substitution in monoaqua cations $Cp^*Ir(A-B)(H_2O)^{2+/+}$ and in the triaqua cation **1** by pyridine at 298 K

Aqua cation	pH	k_L [$M^{-1}s^{-1}$]	k_{-L} [s^{-1}][a]	$K = k_L/k_{-L}$ [M^{-1}]	K [M^{-1}][b]
4	4.8	6270 ± 90	–	–	–
	2.0	6270 ± 330	0.008 ± 0.004	$(7.8 \pm 4.4) \times 10^5$	$(8.7 \pm 0.7) \times 10^5$
6	2.0	643 ± 15	–[c]	–	–
7	4.8	63 ± 0.8	–[c]	–	–
	2.0[d]	79 ± 1.0	0.0053 ± 0.0004	$(0.15 \pm 0.01) \times 10^5$	$(0.15 \pm 0.01) \times 10^5$
2	4.8	41.6 ± 0.7	0.0025 ± 0.0009[d]	$(0.17 \pm 0.07) \times 10^5$	–
	2.0[d]	44.2 ± 0.5	0.0008 ± 0.0003	$(0.5 \pm 0.2) \times 10^5$	$(0.41 \pm 0.02) \times 10^5$
8	4.8	16.9 ± 0.6	0.004 ± 0.001	4225 ± 1200	–
5	4.8	10.5 ± 0.3	–[c]	–	–
1	2.0	2610 ± 40[e]	–	–	–

[a] According to Equation (7), rate constant k_{-L} corresponds to the intercept of the plot of k_{obsd} vs. [L]; in most cases, the values of k_{-L} are therefore obtained with high error limits. – [b] As obtained from the amplitude ΔA according to Equation (8). – [c] Error limits too high to accept data for k_{-L} as sufficiently reliable. – [d] Substitution studied with py-nia[21] instead of py. – [e] First substitution step; data taken from ref.[9]

$$\Delta A = A_\infty K[py]_{tot}/(1 + K[py]_{tot}) \qquad (8)$$

The values of k_L, k_{-L}, and K obtained are summarized in Table 6.

The data for the system **4**/py demonstrate that the pH value has no effect on k_L, which clearly indicates that in solutions at pH = 2.0 and 4.8 the reacting iridium species is the same. This is in line with the UV absorption data (see Table 2). Within the error limits, equilibrium constant $K = 7.8 \times 10^5$ M^{-1}, as obtained according to $K = k_L/k_{-L}$, is in good agreement with $K = 8.7 \times 10^5$ M^{-1}, as derived from the dependence of ΔA on $[py]_{tot}$ according to the relationship in Equation (8). It is noteworthy that the substitution of water in the proline complex by py is a monophasic process, properly described by a single exponential function. In agreement with the UV absorption data, this finding supports the interpretation that the trinuclear compound **3b** is hydrolyzed to form the monoaqua cation **4** when dissolved in water.[30] If the trinuclear cation **3** were to be present in solution, one should observe biphasic or even triphasic kinetic behaviour.

As described above, the acidity of the coordinated water in the species $Cp^*Ir(A-B)(H_2O)^{2+/+}$ is not significantly affected by the nature of A–B (see Table 3). In contrast to this lack of dependence, the magnitude of the rate constant k_L clearly depends on A–B (see Table 6). The proline complex **4** (k_L = 6270 $M^{-1}s^{-1}$) reacts faster than the bipyridine complex **5** (k_L = 10.5 $M^{-1}s^{-1}$) by a factor in excess of 500. As a general rule, it is found that the singly charged complex cations (A–B = prol and picac) react more rapidly than the doubly charged ones (A–B = dpen, dach, phen, and bpy). However, the difference of a factor of 10 between the k_L data for **4** and the picolinic acid complex **6** clearly shows that the charge on the cations is not the only rate-determining parameter.

The reverse reaction is less affected by the nature of A–B. The values obtained for the rate constant k_{-L} only vary between 0.008 s^{-1} and 0.0008 s^{-1}. As a result of the effects of A–B on k_L and k_{-L}, the overall equilibrium constant K ranges from 7.8×10^5 M^{-1} (A–B = prol) to 4.2×10^3 M^{-1} (A–B = phen).

Due to pH-dependent protonation of the incoming pyridine ligand, rate constant k_{-L} for the reverse reaction was not reliably accessible for some of our complexes under certain conditions (see Table 6). Experiments in which the less basic pyridine derivative py-nia (= nicotinamide; pK_a = 3.47[29]), rather than pyridine (pK_a = 5.26[29]), was treated with $Cp^*Ir(R,R\text{-dpen})(H_2O)^{2+}$ (**7**) and **2** at pH = 2.0 led to reliable data for k_{-L} and K. Further evidence for the reversibility of substitution reaction according to Equation (3) was provided by the results of some pH-jump stopped-flow experiments performed on the system **2**/py-nia.[31] The change in absorbance with time associated with the pH-jump from pH = 2.0 to proton concentrations $[H^+]$ = 0.27, 0.55, and 1.5 M, respectively, proved to be exponential according to Equation (5). The experimental rate constant k_{obsd}, formally described by Equation (7), was found to be independent of $[H^+]$, with a mean value of $k_{obsd} = (1.02 \pm 0.03) \times 10^{-3}$ s^{-1}.[31] Within the limits of error, this value is in agreement with $k_{-L} = (0.8 \pm 0.3) \times 10^{-3}$ s^{-1} as determined from the kinetics of the complex formation reaction (see Table 6). This means that the pH-jump from pH = 2 to higher proton concentrations causes aquation of the cation $Cp^*Ir(R,R\text{-dach})(\text{py-nia})^{2+}$ according to Equation (9). Due to pyridine protonation at the high proton concentrations employed, the contribution of the rate term $k_L[py]$ in Equation (7) becomes negligibly small.

$$Cp^*Ir(R,R\text{-dach})(\text{py-nia})^{2+} + H_2O \xrightarrow{k_{-L}} Cp^*Ir(R,R\text{-dach})(H_2O)^{2+} + \text{py-nia} \qquad (9)$$

In comparison to other aqueous systems [e.g. $Ni(H_2O)_6^{2+}$/py; K = 81 M^{-1}],[32] the complexes $Cp^*Ir(A-B)L^{2+/+}$ prove to be extraordinarily stable. Since the carbon–iridium bonds are resistant to hydrolysis even in very acidic solutions, high proton concentrations can be used to reduce the concentration of the pyridine ligand. It is thus possible to accurately determine large K values.

Water Substitution in $Cp^*Ir(A-B)(H_2O)^{2+/+}$ Complexes by Thiourea, Dimethyl Sulfide, and Monodentate Anions

The rates of associatively controlled substitution reactions are strongly affected by the nucleophilicity of the incoming ligand L. In the case of associative substitutions at Pt^{II} complexes, the nucleophilic discrimination factor *S*, as obtained from n^{o}_{Pt} values according to Equation (10), is used to quantify this effect of the nucleophilicity of L on the rate of the reaction (*k* = second-order substitution rate constant; n^{o}_{Pt} = empirical measure of the nucleophilicity).[33]

$$\log k = S n^{o}_{Pt} + c \qquad (10)$$

To obtain information on the mechanism of water substitution according to Equation (3), the rate constant k_L was determined for the entry of various ligands L into the monoaqua complexes $Cp^{*}Ir(A-B)(H_2O)^{2+/+}$. Under pseudo-first-order conditions ($[L]_o \geq 10 \times [complex]_o$), substitution was found to be a practically irreversible process with the (*A*,*t*) data conforming to Equation (5). The dependence of k_{obsd} on $[L]_o$ according to Equation (6), led to the k_L data summarized in Table 6. Analysis of these data shows that (i) as found for L = py, water substitution at the various cations $Cp^{*}Ir(A-B)(H_2O)^{2+/+}$ by TU and DMS is more than two orders of magnitude faster for the singly charged proline and picolinic acid complexes than for the bipyridine complex, (ii) for a given cation $Cp^{*}Ir(A-B)(H_2O)^{2+/+}$, the magnitude of k_L follows the order TU > DMS > py, and (iii) water substitution at the cations **2** and **5** by the anions Br^-, I^-, SCN^-, N_3^-, and NO_2^- is faster than that by the neutral ligands TU, DMS, and py. The latter result is in line with expectation for charge effects according to the Eigen−Wilkins mechanism.[34]

A plot of log k_L vs. n^{o}_{Pt} for L = py, DMS, and TU is shown in Figure 5. It can be seen that the substitution rate constant k_L increases with increasing nucleophilicity of L, as characterized by the parameter n^{o}_{Pt}. This increase of k_L with n^{o}_{Pt} is found for all of the $Cp^{*}Ir(A-B)(H_2O)^{2+/+}$ complexes studied. The nucleophilic discrimination factor *S* ranges from 0.25 for the proline complex **4** to 0.41 for the *R*,*R*-dach complex **2**. In line with the second-order rate law obtained for substitution reaction according to Equation (3), this finding excludes a *D* mechanism. However, for typical associative substitutions at Pt^{II} complexes (*A* mechanism) it is found that *S* ranges from 0.6 to 1.4.[33] This im-

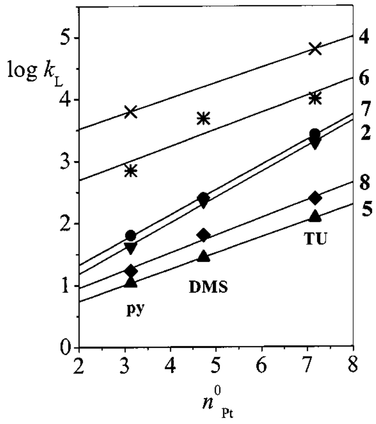

Figure 5. Dependence of rate constant k_L on the nucleophilicity of the neutral ligands py, DMS, and TU (**4**, *S* = 0.25; **6**, *S* = 0.27 ± 0.10; **7**, *S* = 0.40 ± 0.01; **2**, *S* = 0.41 ± 0.02; **8**, *S* = 0.28 ± 0.01; **5**, *S* = 0.26 ± 0.01)

Table 7. Second-order rate constant k_L ($M^{-1}s^{-1}$) for water substitution in monoaqua cations $Cp^{*}Ir(A-B)(H_2O)^{2+/+}$ and in the triaqua cation **1** by monodentate ligands L according to Equation (3) under pseudo-first-order conditions at 298 K and *I* = 0.2 M

Cation	pH	Entering ligand L						
		TU[a][21]	DMS[21]	Br^-	I^-	N_3^-	NO_2^-	SCN^-
2	2.0	1960 ± 50	143 ± 5	8830 ± 260	(1.39 ± 0.04) × 10^4	–	3730 ± 110[c]	(1.19 ± 0.04) × 10^4 [c]
7	2.0	2650 ± 60	252 ± 7	–	–	–	–	–
4	2.0	(6.4 ± 0.2) × 10^4 [b]	–	–	–	–	–	–
6	2.0	(1.00 ± 0.04) × 10^4	4880 ± 160	–	–	–	–	–
8	2.0	244 ± 7	63.6 ± 2	–	–	–	–	–
5	2.0	120 ± 4	27.8 ± 1	110 ± 6[c] [d] [e]	285 ± 15[c−e]	181 ± 9[c−e]	–	342 ± 20[c−e]
1[f]	2.0	8660 ± 30	3990 ± 20	(1.34 ± 0.1) × 10^4	(2.5 ± 0.1) × 10^4	–	–	(8.8 ± 0.4) × 10^4

[a] $[L]_o \geq 10 \times [complex]_o$. − [b] As obtained under stoichiometric conditions. − [c] As obtained at pH = 4.8. − [d] Data taken from ref.[7] − [e] Data determined at *I* = 0.3 M. − [f] First substitution step; data, as taken from ref.[9], refer to the substitution of 1 water molecule in **1**.

Table 8. Rate and activation parameters for water substitution in monoaqua cations $Cp^{*}Ir(A-B)H_2O^{2+/+}$ and in the triaqua cation **1** according to Equation (3) at *I* = 0.2 M and pH = 2.0

Aqua cation	Nucleophile L[a]	k_L^{298} [M^{-1} s^{-1}]	$\Delta H^{\neq}$ [kJ mol^{-1}]	$\Delta S^{\neq}$ [J K^{-1} mol^{-1}]	$\Delta V^{\neq}$ [cm^3 mol^{-1}]	Ref.
5	TU	120 ± 4	59 ± 5[b]	+4 ± 9[b]	+2.3 ± 0.5[c]	this work
2	TU	1960 ± 50	63 ± 2	+26 ± 5	+7.4 ± 0.4[d]	this work
6	TU	(10.0 ± 0.4) × 10^3	53 ± 2	+12 ± 4	+7.3 ± 0.4[d]	this work
1	Cl^-	(5.2 ± 0.1) × 10^3	62 ± 2	+35 ± 6	+4.7 ± 0.4[e]	[9]
	Br^-	(13.4 ± 0.3) × 10^3	55 ± 1	+18 ± 4	+3.9 ± 0.3[e]	[9]
	py−CN	(12.3 ± 0.2) × 10^2	–	–	+4.4 ± 0.4[e]	[9]
	py-nia	(17.7 ± 0.2) × 10^2	–	–	+5.4 ± 0.4[e]	[9]

[a] For abbreviations, see ref.[21] − [b] Data taken from ref.[7] − [c] *T* = 293 K. − [d] *T* = 288 K. − [e] *T* = 298 K.

plies that the substitution reactions under study have a rather weak dependence on the nucleophilicity of L.

Activation Parameters

The kinetics of water substitution at three monoaqua $Cp^*Ir(A-B)(H_2O)^{2+/+}$ cations by thiourea were studied at various temperatures and pressures. The corresponding activation parameters, along with related literature data, are listed in Table 8.

The values obtained for $\Delta H^{\neq}$, $\Delta S^{\neq}$, and $\Delta V^{\neq}$ are rather similar in magnitude for all three complexes. When compared to the data obtained for water substitution at the triaqua species **1**[9] and to corresponding data reported in the literature,[35−37] the positive volume of activation, which ranges from $\Delta V^{\neq} = +2.3$ cm^3 mol^{-1} for **5** to $\Delta V^{\neq} = +7.4$ cm^3 mol^{-1} for **2**, suggests the operation of a dissociatively controlled interchange mechanism (I_d). In line with the hypothesis of an I_d mechanism, the activation entropies listed in Table 8 are all positive and small. It is interesting to note that the activation volumes for the complexes **2** and **6** are significantly more positive than that for complex **5**. In the former cases, water substitution by thiourea is considerably faster, which may point to a more dissociative process than in the case of complex **5**. By way of comparison, the activation volumes quoted for water substitution at the triaqua complex **1** by a variety of nucleophiles vary between +3.9 and +5.4 cm^3 mol^{-1}, again typical for an I_d mechanism. All of these reactions are many orders of magnitude faster than water exchange and ligand substitution at hexaaqua iridium(III), which is characterized by a negative volume of activation as befits an I_a mechanism.[10,21] The significant labilization caused by the Cp* ligand is expected to result in a ground-state lengthening of the $Ir-OH_2$ bond (see earlier discussion). Compared to the case without ground-state labilization, this, in turn, will require a lesser degree of bond breakage (and a smaller volume increase) in going to a dissociative transition state. Therefore, in the absence of structural information on the Ir−O(water) bond lengths in all of the complexes appearing in Table 8, the reported volumes of activation do not rule out the operation of a limiting *D* mechanism.

Conclusions

Comparison of a series of half-sandwich monoaqua complexes $Cp^*Ir(A-B)(H_2O)^{2+/+}$ with the triaqua species **1** has shown that the acidity of the coordinated water in the pseudo-octahedral cations $Cp^*Ir(A-B)(H_2O)^{2+/+}$ is more than three orders of magnitude less than that in **1**. It follows from kinetic investigations of the substitution of water in the monoaqua complexes $Cp^*Ir(A-B)(H_2O)^{2+/+}$ by monodentate ligands L that the formation of the species $Cp^*Ir(A-B)L^{2+/+}$ is a second-order reaction, rate = k_L[complex][L]. The magnitude of the complex formation rate constant k_L is affected by the nature of both the bidentate ligand A−B and ligand L. For a given incoming ligand L, it is found that k_L is smallest for complexes with σ-donor/π-acceptor N,N ligands (bpy and phen), somewhat greater for those with σ-donor N,N ligands (*R*,*R*-dach and *R*,*R*-dpen), and greatest for those with σ-donor N,O^- ligands (picac and prol). The reactivity of complex **6** is lower compared to that of **4**, which is probably due to the π-acceptor properties of the pyridine ring. For a given $Cp^*Ir(A-B)(H_2O)^{2+/+}$ complex, it is found that k_L increases with the nucleophilicity of L, as characterized by the empirical parameter n^o_{Pt}. The effect of L on the second-order rate constant k_L is very similar to the effect of the incoming ligand on the rate of water substitution in the triaqua complex **1**. The overall kinetic data suggest that water substitution in the species $Cp^*Ir(A-B)(H_2O)^{2+/+}$ follows an I_d mechanism.

Ligand substitution is thus mainly governed by the lability of the leaving water molecule. For L = py, the rate of aquation (rate constant k_{-L}) is less affected by the nature of A−B than the rate of water substitution (rate constant k_L). From the values of k_{-L}, it therefore follows that the lability of the coordinated pyridine is roughly of the same order of magnitude for all the $Cp^*Ir(A-B)(py)^{2+/+}$ complexes. The pronounced differences in the lability of the coordinated water are possibly a consequence of its limited polarizability or "hardness". As a general rule, it is found that the iridium centre in the monoaqua species $Cp^*Ir(A-B)(H_2O)^{2+/+}$ as well as in the triaqua cation **1** favours polarizable or "soft" ligands, so as to form kinetically and thermodynamically stable complexes.

Experimental Section

Unless stated otherwise, all manipulations were performed under aerobic conditions using commercial-grade solvents. The metal salts, organic solvents, and ligands (reagent grade) were obtained from commercial sources and were used without further purification. $[Cp^*IrCl_2]_2$ was synthesized according to published procedures.[38] Deionized water was doubly distilled in a quartz apparatus prior to use.

General Procedure for the Preparation of the Complexes: Portions of 0.100 g (0.126 mmol) of $[Cp^*IrCl_2]_2$ were suspended in methanol (5 mL) and 2 equiv. of the bidentate ligand A−B were added at ambient temperature to immediately produce a clear yellow solution. After stirring for 3 h, the solvent was evaporated. The residue was redissolved in water (7 mL) and the resulting solution was heated to ca. 80 °C. A solution of 4 equiv. (0.504 mmol) of $AgClO_4$ in water (5 mL) was added to the acidified solution (pH = 2−3, $HClO_4$) to remove chloride by precipitation of AgCl, which was separated by hot filtration after stirring for 2 h. The solvent was partially evaporated until crystallization occurred. The addition of 1 equiv. of $NaClO_4$ completed the crystallization. − To achieve deprotonation in the case of the ligands picac and prol,[21] following the addition of the ligand A−B, a stoichiometric amount of triethylamine was added to the reaction mixture. − ***Caution:*** Perchlorate salts are potentially explosive; they should be handled with care and in small portions only!

2b: Yellow needles from water (pH = 2−3, $HClO_4$). − Yield 0.118g (69%). − $C_{16}H_{33}Cl_2IrN_2O_{10}$ (676.57): calcd. C 28.40, H 4.92, N 4.14; found C 28.01, H 4.56, N 4.08. − ^1H NMR (D_2O): δ = 1.05−1.46 (m, 4 H, cycl.-H), 1.51−1.66 (m, 2 H, cycl.-H), 1.71 (s, 15 H, Cp*), 2.00−2.07 (m, 4 H, cycl.-H). − IR (KBr): $\tilde{\nu}$ = 3288 [m, ν(N−H)], 3254 [m, ν(N−H)], 2943 (m), 2862 (w), 1458 (w), 1386 (w), 1089 (vs), 625 (s) cm^{-1}.

3b: Yellow prisms from water (pH = 2−3, $HClO_4$). − Yield 0.088g (64%). − $(C_{15}H_{23}ClIrNO_6)_3$ (1622.97): calcd. C 33.30, H 4.28, N 2.59; found C 31.32, H 4.02, N 2.48. − ^{1}H NMR (D_2O): δ = 1.78 (s, 15 H, Cp*), 1.86−2.14 (m, 3 H, cycl.-H), 2.41 (m, 1 H, cycl.-H), 3.12 (s, 1 H, cycl.-H), 3.33 (m, 1 H, cycl.-H), 4.05 (t, 1 H, α-H). − IR (KBr): $\tilde{\nu}$ = 3227 [s, ν(N−H)], 2970 (m), 1575 [s, ν(C=O)], 1445 (m), 1385 (m), 1095 (vs), 930 (s), 623 (m) cm^{-1}.

5b: Yellow needles from water (pH = 2−3, $HClO_4$). Yield 0.123 g (72%). − $C_{20}H_{25}Cl_2IrN_2O_9$ (700.55): calcd. C 34.29, H 3.60, N 4.00; found C 33.50, H 3.01, N 3.96. − ^{1}H NMR (D_2O): δ = 1.58 (s, 15 H, Cp*), 7.74 (m, 2 H, Ar-H), 8.17 (m, 2 H, Ar−H), 8.42 (d, 2 H, Ar−H), 8.85 (d, 2 H, Ar−H). − IR (KBr): $\tilde{\nu}$ = 3086 (s), 3121 (s), 2920 (m), 1608 (m), 1466 (m), 1446 (m), 1096 (vs), 772 (s), 625 (s) cm^{-1}.

6b: Yellow prisms from water (pH = 2−3, $HClO_4$). − Yield 0.099g (71%). − $(C_{16}H_{19}ClIrNO_6)_3$ (1647.01): calcd. C 35.00, H 3.49, N 2.55; found C 32.67, H 3.84, N 2.76. − ^{1}H NMR (D_2O): δ = 1.77 (s, 15 H, Cp*), 8.01 (m, 1 H, Ar−H), 8.22 (m, 1 H, Ar−H), 8.38 (m, 1 H, Ar−H), 9.09 (m, 1 H, Ar−H). − IR (KBr): $\tilde{\nu}$ = 1614 (w), 1583 (m), 1547 [s, ν(C=O)], 1475 (m), 1406 (m), 1381 (w), 1335 (w), 1298 (w), 1265 (w), 1093 (vs), 1032 (m), 766 (m), 710 (m), 690 (m), 623 (w) cm^{-1}.

7b: Yellow powder from water (pH = 2−3, $HClO_4$). − Yield 0.136g (70%). − $C_{24}H_{35}Cl_2IrN_2O_{10}$ (774.68): calcd. C 37.21, H 4.55, N 3.62; found C 35.52, H 4.26, N 3.51. − ^{1}H NMR (D_3COD): δ = 1.85 (s, 15 H, Cp*), 3.97 (d, 1 H, ^3J = 12.3 Hz, C−H), 4.56 (d, 1 H, ^3J = 12.3 Hz, C−H), 7.28 (m, 10 H, Ar−H). − ^{1}H NMR (D_2O): δ = 1.77 (s, 15 H, Cp*), 4.17 (s, 2 H, C−H), 7.28 (s, 10 H, Ar−H). − IR (KBr): $\tilde{\nu}$ = 3290 [m, ν(N−H)], 3240 [m, ν(N−H)], 3153 (m), 3066 (m), 3033 (m), 2025 (w), 1884 (w), 1813 (w), 1589 (m), 1498 (m), 1456 (m), 1388 (m), 1093 (vs), 700 (s), 625 (s), 577 (m), 498 (m) cm^{-1}.

8b: Yellow crystals from water (pH = 2−3, $HClO_4$). − Yield 0.137 g (75%). − $C_{22}H_{27}Cl_2IrN_2O_9$ (726.59): calcd. C 36.47, H 3.34, N 3.87; found C 36.58, H 3.35, N 4.18. − ^{1}H NMR ([D$_6$]DMSO): δ = 1.70 (s, 15 H, Cp*), 8.35 (m, 4 H, Ar−H), 9.14 (d, 2 H, Ar−H), 9.45 (d, 2 H, Ar−H). − IR (KBr): $\tilde{\nu}$ = 3091 (w), 3061 (w), 1430 (m), 1090 (vs), 845 (s), 718 (m), 625 (s) cm^{-1}.

Instrumentation: UV/Vis spectra: diode-array spectrophotometer (Zeiss Specord S10); NMR spectra: FT NMR spectrometer (Bruker AM 200 and WM 300); IR spectra: FT-IR spectrometer (Nicolet Impact 400); pH measurements: glass electrode (Schott) in combination with a potentiometer (Metrohm 691), calibrated at I = 0.1 M ($NaNO_3$) and 25 °C to yield $-\log[H^+]$ = pH − 0.09; kinetics of reaction according to Equation (3): multi-wavelength stopped-flow spectrophotometer (J. & M., TIDAS)[39] and stopped-flow spectrophotometer in combination with a high-pressure cell.[40]

Spectrophotometric Titrations: The dissociation of the monoaqua complexes Cp*Ir(A−B)(H$_2$O)$^{2+/+}$ according to Equation (4) was monitored by spectrophotometric titrations of acidic solutions of the complexes with 0.1 M NaOH. Least-squares fitting of Equation (11) to the (absorbance,[H$^+$]) data led to the acid dissociation constants K_a (A_{H2O} and A_{OH} refer to the absorbances of the aqua and hydroxy complexes, respectively, at the concentration [complex]$_{tot}$).

$$A = (A_{OH} + A_{H2O}[H^+]/K_a)/(1 + [H^+]/K_a) \qquad (11)$$

Kinetic Measurements: The reaction according to Equation (3) was monitored in freshly prepared aqueous solutions in the wavelength range 200−500 nm under pseudo-first-order conditions ($[L]_o \geq 10 \times [complex]_o$) at various temperatures (285−318 K) and pressures (10−150 MPa). The ionic strength was fixed at I = 0.2 M ($NaClO_4$ or $NaNO_3$). Measurements were made at either pH = 2 (as adjusted with $HClO_4$) or 4.8 (as adjusted with the noncoordinating buffer 2,6-dimethylpyridine-3-sulfonic acid[41]). Least-squares fitting of the (absorbance,time) data with Equation (5) led to the experimental rate constant k_{obsd}, which is defined by Equations (6) and (7) for irreversible and reversible pseudo-first-order reactions, respectively. Rate constants k_L and k_{-L} were obtained from the dependence $k_{obsd} = f([L]_o)$ according to Equations (6) and (7), respectively. The amplitude ΔA in Equation (5) depends on $[L]_o$ according to Equation (8). Fitting of this Equation to the (ΔA,$[L]_o$) data led to the equilibrium constant $K = k_L/k_{-L}$. − The volume of activation was obtained from the pressure dependence of k_{obsd} according to Equation (12). A correction for the pressure dependence of the activity coefficients (less than 0.6 cm^3 mol^{-1} under the given conditions[42]) was not applied.

$$\Delta V^{\neq}_{exptl} = -RT\,(\partial \ln k_{obsd}/\partial P)_T \qquad (12)$$

Crystallography: The crystals were obtained from aqueous solutions (pH = 2−3, $HClO_4$) as stated above. Measurements were made with a four-circle diffractometer (STOE-STADI-4) using graphite-monochromated Mo-K_α radiation (λ = 0.71069 Å); scan 2θ:ω = 1:1. Cell constants were determined by the least-squares method from the 2θ angles of 58 and 54 reflections for **2b** and **3b**, respectively. The structures were solved by direct methods with SHELXS-86 and refined by least squares to the R values given in Table 9 using the program package SHELXL-93. The non-hydrogen atoms were refined anisotropically. All hydrogen atoms were placed in their calculated positions. Crystal data and data collection parameters are listed in Table 9; selected bond lengths and

Table 9. Crystallographic data for complexes **2b** and **3b**

	2b	**3b**
Empirical formula	$C_{16}H_{33}Cl_2IrN_2O_{10}$	$C_{15}H_{23}ClIrNO_6$
Crystal system	monoclinic	hexagonal
Space group	$P2_1$	$P6_3$
a/Å	12.628(4)	17.766(3)
b/Å	9.462(3)	17.766(3)
c/Å	20.654(6)	11.736(3)
β/°	95.67(1)	90
V/Å^3	2455.8(13)	3208.0(11)
Z	4	6
Molecular mass	676.54	540.99
Measured reflections	9569	4728
Independent reflections	8603	4195
T/K	300(2)	300(2)
λ/Å	0.71069	0.71069
$D_{calcd.}$/gcm^{-3}	1.830	1.680
μ/mm^{-1}	5.705	6.393
$R1$[a] [$I > 2\sigma(I)$]	0.0266	0.0356
$wR2$[b]	0.0661	0.0826
Residual electron density/eÅ^{-3}	0.590/−0.483	1.055/−0.674
Absorption correction	numerical T_{min} = 0.173 T_{max} = 0.391	numerical T_{min} = 0.347 T_{max} = 0.403
Absolute structure parameter	0.071(12)	0.00(2)

[a] $R1 = \Sigma|F_o| - |F_c|/\Sigma|F_o|$. − [b] $wR2 = (\Sigma[w(F_o^2 - F_c^2)^2]/\Sigma[w(F_o^2)^2])^{1/2}$, where $w = 1/[\sigma^2(F_o^2) + qP^2 + jP]$ $\{q = 0.0496$, $j = 4.4892$ for [Cp*Ir(D-prol)]$_3$(ClO$_4$) and $q = 0.0327$, $j = 4.3163$ for [Cp*Ir(R,R-dach)H$_2$O](ClO$_4$)$_2$·H$_2$O; $P = (F_o^2 + 2\,F_c^2)/3\}$.

angles are given in Table 3 and 4. Crystallographic data (excluding structure factors) for the structures reported in this paper have been deposited with the Cambridge Crystallographic Data Centre as supplementary publication nos. CCDC-146445 (**3b**) and -146446 (**2b**). Copies of the data can be obtained free of charge on application to the CCDC, 12 Union Road, Cambridge CB2 1EZ, U.K. [Fax: (internat.) + 44-1223/336-033; E-mail: deposit@ccdc.cam.ac.uk].

Supporting Information: UV/Vis spectroscopic data (Figures S1−S3, S6), spectrophotometric titration data (Figures S4, S5), observed rate constants at various concentrations, temperatures, and pressures (Tables S1−S26, Figures S7, S8; see also the footnote on the first page of this paper).

Acknowledgments

Sponsorship of this work by the Deutsche Forschungsgemeinschaft and the Verband der Chemischen Industrie e.V. is gratefully acknowledged. A sample of iridium(III) chloride was kindly provided by Degussa−Hüls AG.

---

[1] U. Koelle, *Coord. Chem. Rev.* **1994**, *135/136*, 623−650.

[2] M. S. Eisen, A. Haskel, H. Chen, M. M. Olmstead, D. P. Smith, M. F. Maestre, R. H. Fish, *Organometallics* **1995**, *14*, 2806−2812.

[3] S. Ogo, H. Chen, M. M. Olmstead, R. H. Fish, *Organometallics* **1996**, *15*, 2009−2013.

[4] S. Ogo, O. Buriez, J. B. Kerr, R. H. Fish, *J. Organomet. Chem.* **1999**, 66−74.

[5] R. H. Fish, *Coord. Chem. Rev.* **1999**, *185−186*, 569.

[6] S. Ogo, N. Makihara, Y. Watanabe, *Organometallics* **1999**, *18*, 5470−5474.

[7] L. Dadci, H. Elias, U. Frey, A. Hörnig, U. Koelle, A. E. Merbach, H. Paulus, J. S. Schneider, *Inorg. Chem.* **1995**, *34*, 306−315.

[8] R. Boca, H. Elias, *Polyhedron* **1996**, *15*, 2425−2431.

[9] S. Cayemittes, T. Poth, M. J. Fernandez, P. G. Lye, M. Becker, H. Elias, A. E. Merbach, *Inorg. Chem.* **1999**, *38*, 4309−4316.

[10] A. Cusanelli, U. Frey, D. T. Richens, A. E. Merbach, *J. Am. Chem. Soc.* **1996**, *118*, 5265−5271.

[11] M. Stebler-Röthlisberger, W. Hummel, P. A. Pittet, H. B. Bürgi, A. Ludi, A. E. Merbach, *Inorg. Chem.* **1988**, *27*, 1358−1363.

[12] A. Cusanelli, L. Nicula-Dadci, U. Frey, A. E. Merbach, *Chimia* **1996**, *50*, 618−620.

[13] The chemistry of the corresponding monoaqua rhodium species $Cp^*Rh(A{-}B)(H_2O)^{2+/+}$ has been dealt with in some detail: [13a] R. P. Hughes, D. C. Lindner, A. L. Rheingold, L. M. Liable-Sands, *J. Am. Chem. Soc.* **1997**, *119*, 11544−11545. − [13b] P. M. Boyer, C. P. Roy, J. M. Bielski, J. S. Merola, *Inorg. Chim. Acta* **1996**, *245*, 7−15. − [13c] D. Carmona, C. Cativiela, R. Garcia-Correas, F. J. Lahoz, M. P. Lamata, J. A. Lopez, M. P. Lopez-Ram de Viu, L. A. Oro, E. Dan Jose, F. Viguri, *Chem. Commun.* **1996**, 1247−1248.

[14] D. Carmona, F. J. Lahoz, S. Elipe, L. A. Oro, M. P. Lamata, F. Viguri, C. Mir, C. Cativiela, M. P. López-Ram de Víu, *Organometallics* **1998**, *17*, 2986−2995.

[15] D. Carmona, F. J. Lahoz, R. Atenico, L. A. Oro, M. P. Lamata, F. Viguri, E. San José, C. Vega, J. Reyes, F. Joó, Á. Kathó, *Chem. Eur. J.* **1999**, *5*, 1544−1564.

[16] K. Mashima, T. Abe, K. Tani, *Chem. Lett.* **1998**, 1199−1200.

[17] K. Mashima, T. Abe, K. Tani, *Chem. Lett.* **1998**, 1201−1202.

[18] K. Murata, T. Ikariya, *J. Org. Chem.* **1999**, *64*, 2186−2187.

[19] M. J. Palmer, M. Wells, *Tetrahedron: Asymmetry* **1999**, *10*, 2045−2061.

[20] K. Severin, R. Bergs, W. Beck, *Angew. Chem.* **1998**, *110*, 1722−1743; *Angew. Chem. Int. Ed.* **1998**, *37*, 1634−1654.

[21] Abbreviations used: Cp* = pentamethylcyclopentadienyl anion; phen = 1,10-phenanthroline; bpy = 2,2′-bipyridine; dpen = 1,2-diphenylethylenediamine; dach = 1,2-diaminocyclohexane; picac = anion of picolinic acid; prol = anion of proline; py = pyridine; py-nia = nicotinamide; py-CN = 4-cyanopyridine; DMS = dimethyl sulfide; TU = thiourea; I_d = dissociatively controlled interchange; I_a = associatively controlled interchange.

[22] K. Isobe, B. M. Baily, P. M. Maitlis, *J. Chem. Soc., Dalton Trans.* **1981**, 2003−2008.

[23] O. Almog, A. Bino, D. Garfinkel-Shweky, *Inorg. Chim. Acta* **1993**, *213*, 99−102.

[24] F. Galsbol, S. Larsen, B. Rasmussen, J. Springborg, *Inorg. Chem.* **1986**, *25*, 290−297.

[25] R. Krämer, K. Polborn, Ch. Robl, W. Beck, *Inorg. Chim. Acta* **1992**, *198*, 415−420.

[26] K. Sünkel, W. Hoffmüller, W. Beck, *Z. Naturforsch.* **1998**, *53b*, 1365−1368.

[27] One has to consider that at pH = 2.0 most of the pyridine base is protonated [pK_a(py) = 5.26[29]] and the low concentration of the incoming ligand L = py enables interference of the reverse reaction.

[28] To obtain the rate constant k_L from the slope m of the linear dependencies shown in Figure 4a, one has to correct for partial protonation of the pyridine according to $k_L = m\{1 + [H^+]/K_a[py]_0\}$.

[29] A. E. Martell, R. M. Smith, *Critical Stability Constants*, vol. 2, Plenum Press, New York, **1974**.

[30] The UV spectrum of a solution of **3b** in methanol clearly differs from that in water, which suggests that, in contrast to the situation in water, the trinuclear structure is preserved in methanol. This would be in line with the results reported by Carmona et al.,[15] which showed that in solutions of the complexes $[Cp^*Ir(aa)_3](BF_4)_3$ (aa = α-amino acid anion) in dichloromethane, acetone, or methanol, the complexes remain trinuclear.

[31] The pH-jump stopped-flow experiments were carried out by loading one syringe with the solution of the complex ([**2**] = 0.4×10^{-4} M, [py-nia] = 1×10^{-3} M, [$HClO_4$] = 0.01) and the other with acid ([$HClO_4$] = 0.53 M, 1.1 M, and 3.0 M, respectively). The (A,t) data for the decrease of absorbance at 300 nm were fitted with Equation (5), which led to $k_{obsd} = (1.049 \pm 0.004) \times 10^{-3}$ s^{-1} ([$HClO_4$] = 0.27 M), $k_{obsd} = (0.992 \pm 0.003) \times 10^{-3}$ s^{-1} ([$HClO_4$] = 0.55 M), and $k_{obsd} = (1.02 \pm 0.01) \times 10^{-3}$ s^{-1} ([$HClO_4$] = 1.5 M).

[32] M. S. Sun, D. G. Brewer, *Can. J. Chem.* **1967**, *45*, 2729−2739.

[33] M. L. Tobe, *Inorganic Reaction Mechanisms: Studies in Modern Chemistry*, Nelson, London, **1972**, p. 52.

[34] The Eigen−Wilkins mechanism postulates for ligand substitution reactions such as the reaction according to Equation (3) that $k_L = K_{os}k_i$, where K_{os} is the equilibrium constant for fast formation of an outer-sphere complex between $Cp^*Ir(A{-}B)(H_2O)^{2+/+}$ and L, and k_i is the rate constant for rate-controlling ligand interchange in the outer-sphere complex. For electrostatic reasons, K_{os} is greater for cations interacting with anions than for cations interacting with neutral ligands.

[35] A. Drljaca, C. D. Hubbard, R. van Eldik, T. Asano, M. V. Basilevsky, W. J. le Noble, *Chem. Rev.* **1998**, *98*, 2167−2289.

[36] L. Helm, A. E. Merbach, *Coord. Chem. Rev.* **1999**, *187*, 151−181.

[37] R. van Eldik, C. Dücker-Benfer, F. Thaler, *Adv. Inorg. Chem.* **2000**, *49*, 1−58.

[38] C. White, A. Yates, P. M. Maitlis, *Inorganic Synthesis* (Ed.: R. N. Grimes), John Wiley & Sons, New York, **1992**, vol. 29, pp. 228−234.

[39] H. Elias, F. Sattler, K. J. Wannowius, *GIT Fachz. Lab.* **1985**, *29*, 1138.

[40] R. van Eldik, W. Gaede, S. Wieland, J. Kraft, M. Spitzer, D. A. Palmer, *Rev. Sci. Instrum.* **1993**, *64*, 1355.

[41] U. Bips, H. Elias, M. Hauröder, G. Kleinhans, S. Pfeifer, K. J. Wannowius, *Inorg. Chem.* **1983**, *22*, 3862−3865.

[42] R. van Eldik, Y. Kitamura, C. P. Piriz MacColl, *Inorg. Chem.* **1986**, *25*, 4252.

Received June 27, 2000
[I00256]